IEEE Access
Multidisciplinary Rapid Review Open Access Journal

Received 23 June 2022, accepted 16 July 2022, date of publication 20 July 2022, date of current version 27 July 2022.

Digital Object Identifier 10.1109/ACCESS.2022.3192646

RESEARCH ARTICLE

IZO/ITO Double-Layered Transparent Conductive Oxide for Silicon Heterojunction Solar Cells

DOOWON LEE, AHREUM LEE, AND HEE-DONG KIM
Department of Electrical Engineering and Convergence Engineering for Intelligent Drone, Sejong University, Gwangjin-gu, Seoul 05006, South Korea

Corresponding author: Hee-Dong Kim (khd0708@sejong.ac.kr)

This work was supported in part by the Basic Science Research Program through the National Research Foundation of Korea (NRF) funded by the Ministry of Education under Grant NRF-2020R1F1A1048423, and in part by the Korea Institute for Advancement of Technology (KIAT) Grant funded by the Korea Government [Ministry of Trade, Industry and Energy (MOTIE)] through the Competency Development Program for Industry Specialist under Grant P0012451.

ABSTRACT Zinc-doped indium oxide (IZO)+ tin-doped indium oxide (ITO) is proposed in this study as a double-layered transparent conductive oxide (TCO) for the application of silicon heterojunction (SHJ) solar cells. IZO is consecutively deposited via radio frequency sputtering at room temperature. The electrical and optical characteristics of IZO are examined depending on the thickness and the O_2 flow rate, which ranged from 0 to 5 sccm. The improved photocurrent characteristic for the proposed SHJ solar cell with IZO + ITO is achieved from 40.64 to 41.3 mA/cm^2 by an OPAL2 solar cell simulation. The sheet resistance of IZO slightly increases from 120 to 130 Ω/□, which is caused by a decrease in the O_2 vacancy due to an increase in the O_2 flow rate from 1 to 5 sccm. The SHJ solar cells with 4.84 nm IZO deposited at the O_2 flow rate of 4 sccm show the lowest solar weighted reflectance of 4.36%. Therefore, these results indicate that IZO + ITO is expected to increase the efficiency of SHJ solar cells.

INDEX TERMS Light trapping, photovoltaic cells, reflectivity, indium compounds.

I. INTRODUCTION

Levelized cost of energy (LCOE), the amount of power generated over a lifetime of the renewable energy compared to the cost to build the energy source, is an important unit in the renewable energy industry. In order to obtain competitivity of renewable energy compared to other energy sources, a decrease of LCOE on renewable energy is essential. Among the renewable energies, solar cells have attracted attention due to their feasibility for low LCOE. Many types of solar cells have been developed in order to decrease LCOE after the first demonstration of solar cells in 1954, which include (1) crystalline silicon (c-Si), (2) compound semiconductor-based semiconductors, (3) and emerging solar cells, such as organic, dye-sensitized, quantum dot, and perovskite. c-Si solar cells have been intensively studied due to its cost competitiveness. In addition, developments for c-Si solar cells have been accelerated, which is due to the development of integrated circuits. Silicon solar cells can be commonly divided into homojunction and heterojunction solar cells. In the case of homojunction solar cells, passivated emitter and rear solar cells (PERC) and passivated emitter rear locally diffused solar cells (PERL) have been proposed as high-efficiency c-Si solar cells. M. A. Green *et al.* reported PERL with an efficiency of 24.7% on a float zone Si wafer [1]. In addition, M. A. Green also reported PERC with an efficiency of 25.0% [2]. In the case of heterojunction solar cells, silicon heterojunction (SHJ) solar cells have been described as a major technology that needs further development because they allow a high open-circuit voltage (V_{oc}) and fill factor (FF) above 84% [3], [4]. Q. Wang *et al.* reported a VOC of 738 mV and an FF of 84.9% with the SHJ [5], which is higher than PERC with a VOC of 694 mV and an FF of 83.3% [6]. HIT solar cells consist of a c-Si wafer with intrinsic and n/p-type hydrogenated amorphous Si layers (a-Si:H) prior to transparent conducting oxide (TCO) deposition.

The intrinsic a-Si:H layers passivate the c-Si wafer surface well, whereas n/p-type a-Si:H effectively creates a p–n

The associate editor coordinating the review of this manuscript and approving it for publication was Z. G. Zang.

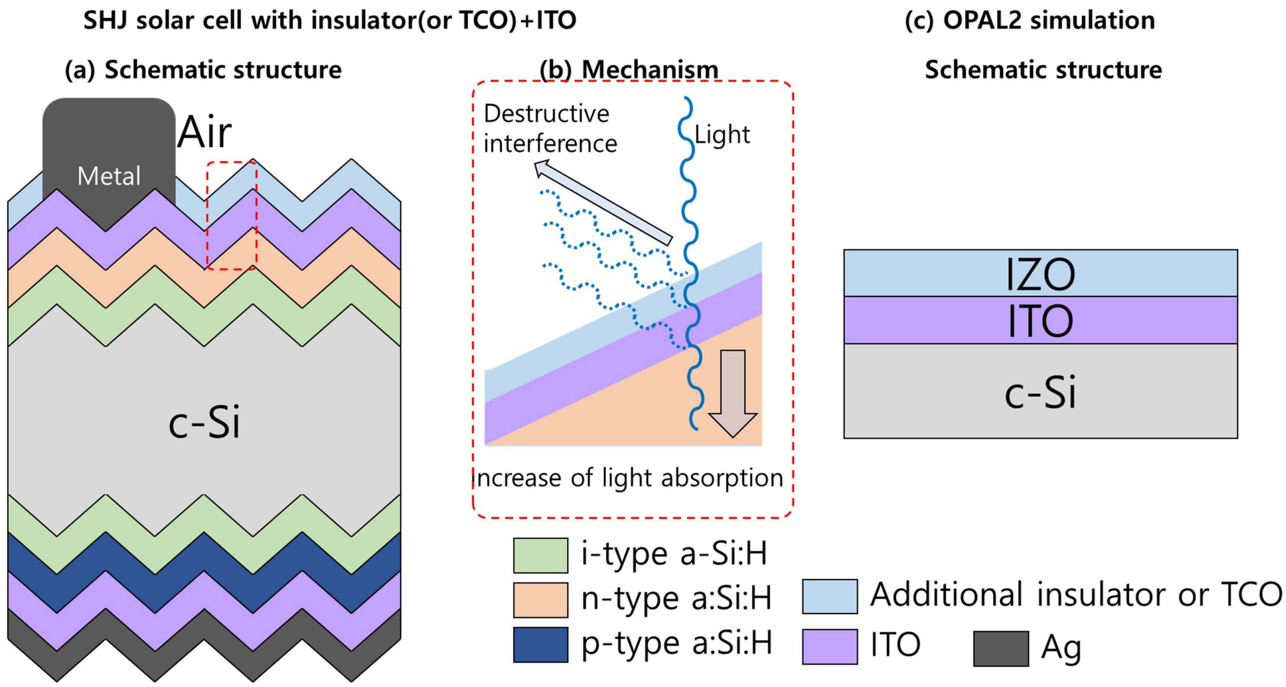

FIGURE 1. SHJ solar cells with an insulator or TCO + ITO, which include the (a) schematic structure, (b) mechanism, and (c) schematic structure of the OPAL2 simulation.

junction. TCO should be deposited as a top electrode of the SHJ solar cells due to the high lateral resistivity of doped a-Si:H. In order to improve the efficiency of SHJ solar cells, technologies that can be used to improve the Voc, FF, and short circuit current density (J_{SC}) of the SHJ solar cells have been studied. S. D. Wolf *et al.* reported that the V_{OC} could be degraded by H_2 effusion from a-Si:H [7]. In addition, Z. C. Holman *et al.* reported that the thickness of a-Si:H is considered for high-efficiency solar cells because thicker a-Si:H causes a decrease of the J_{SC} of solar cells [8]. In order to improve the J_{SC}, studies related to TCOs and structures are proposed by several groups. Tin-doped indium (ITO) is commonly used as the TCO due to its high transmittance and low resistivity below 15 Ω/□, whereas aluminum-doped zinc oxide (AZO) has been proposed as an alternative TCO due its lower cost compared to ITO. A. Cruz *et al.* reported that SHJ solar cells with AZO exhibited superior characteristics compared to the TCO properties of SHJ solar cells with an ITO [9]. Further improvement of J_{SC} has been recently achieved through insulator/TCO structures owing to improved light adsorption in the Si substrate by destructive interference. A. Cruz *et al.* reported that the SiO_2+ TCO layer stack of the SHJ solar cells improved the J_{SC} from 39.6 to 40.4 mA/cm^2, as shown in Figure 1(a), without degradation of the FF [10]. D. Zhang also reported that additional SiO_2 on the top of the ITO improved the J_{SC} to 40.5 mA/cm^2. However, the insulator is deposited on the TCO, so the insulator should be patterned in order to form an electrical connection with a metal line of solar cells, which results in an increase of LCOE. In order to secure a high J_{SC} and low manufacturing cost for a low LCOE, we proposed double TCO layers to improve the J_{SC} [11], [12]. SHJ solar cells with ITO + ITO showed an improved J_{SC} from 40.64 to 41.17 mA/cm^2 [11]. However, we observed that the improvement of the J_{SC} increased as the doping concentration of the ITO decreased, which can deteriorate due to the contact resistivity between the metal contact and the ITO. The high processing temperature for an additional ITO can also deteriorate the efficiency by the destruction of passivation of SHJ solar cell, resulting in an increase of LCOE. In addition, the high price of tin increases the LCOE of the SHJ solar cell. In order to accompany the improvement of efficiency with low manufacturing cost without any thermal stress, additional TCO material on the ITO should be studied. Several types of double-layered TCO were reported by several institutes, such as AZO + ITO, AZO + antimony doped tin oxide (ATO), and ZnO + ITO [11], [13], so the feasibility of the SHJ solar cells with an additional TCO + ITO should be studied for the commercialization of SHJ solar cells. Zinc-doped indium oxide (IZO) has been intensively studied as transistor and TCO resulting from its high mobility and low resistivity [14]–[18]. M. Morales-Masis reported that SHJ solar cells with IZO showed a significant improvement of J_{SC}, which achieved an efficiency above 21.5% [14]. F. Sahli applied IZO to perovskite/silicon tandem solar cells, which achieved a steady-state efficiency of 25.2% [15]. However, the feasibility of IZO + ITO for SHJ solar cells has not been demonstrated. Therefore, zinc-doped indium oxide (IZO) is proposed as

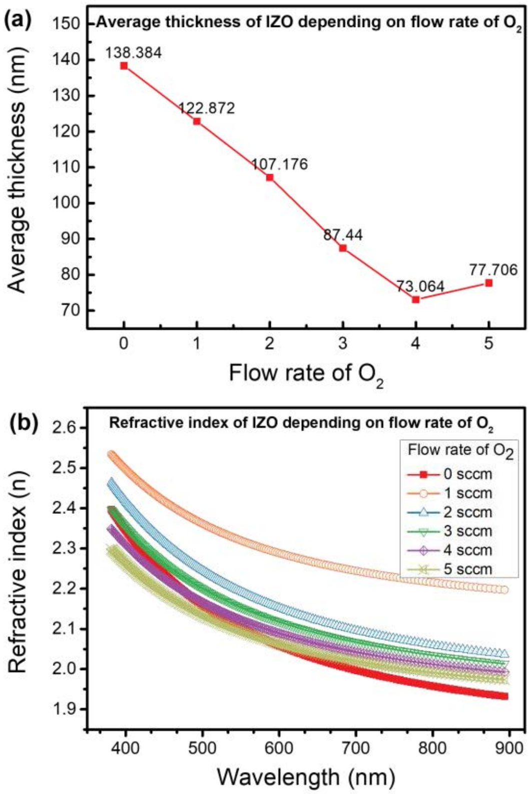

FIGURE 2. Properties of IZO depending on the flow rate of O_2, which include (a) average thickness and (b) refractive index.

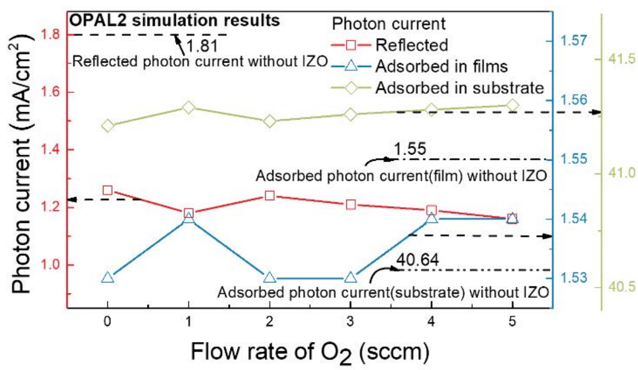

FIGURE 3. Simulation results that present the reflected and adsorbed photon current in the films and substrates via an OPAL2 simulation when the incident photon current was 44 mA/cm^2.

an additional TCO for SHJ solar cells in this paper. The electrical and optical properties of the deposited IZO were first examined. OPAL2 was then used in order to evaluate the adsorbed J_{SC} in the Si substrate with IZO + ITO according to the optical properties of the deposited IZO. After the simulation, the optical properties of SHJ solar cells with IZO + ITO were evaluated. As a result, we observed that the SHJ solar cells with IZO + ITO showed a lower solar weighted reflectance (Rweighted) than the SHJ solar cells without IZO, which indicated that IZO + ITO can improve the J_{SC} of SHJ solar cells.

II. EXPERIMENTS

A. SI SUBSTRATE PREPARATION FOR CHARACTERIZATIONS OF THE IZO

In order to examine the characterization of IZO, the c-Si substrate was first cleaned with acetone, methanol, and deionized water for 15 minutes. The IZO was then deposited using radio frequency (RF) sputtering from an IZO (99.999%) in an Ar/O_2 mixture at RT. The flow rate of the Ar was maintained to 20 sccm, and the O_2 flow rate ranged from 0 to 5 sccm. The sputtering time was 30 minutes. The sputtering chamber was pumped out via a turbo-pump to a working pressure of < 5 mtorr, whereas the sputtering power was maintained at 100 W. The thickness and optical properties of the sputtered IZO were then measured using spectroscopic ellipsometry.

B. SIMULATION OF J_{SC}

In order to evaluate the feasibility of the improved J_{SC} with IZO + ITO, which is the OPAL2 simulation, the structure was defined as shown in Figure 1(b). The N-type c-Si was set as the substrate, and the doping concentration of the sputtered ITO was set to 6.1×10^{20} /cm^3. The randomly upright pyramids with the angle of 54.74° were set as the surface morphology because they are the common structures of solar cells. The solar spectrum and the zenith angle, the angle between the sun and the vertical, were set to AM 1.5g and 0, respectively. In order to calculate the absorbed J_{SC} in the materials, the optical pathlength enhancement factor Z was calculated using $Z = 4 + \{\ln[n^2 + (1 - n^2) \times \exp(-4\alpha W)]\}/\alpha W$, where n is the refractive index, αW is the adsorption coefficient, and W is the thickness of the substrate. The incident photon current was set to 44 mA/cm^2. The J_{SC} of Air/ITO/c-Si was analyzed as a reference prior to evaluating the feasibility of IZO + ITO. The J_{SC} of Air/IZO + ITO/c-Si was then simulated using the optical properties measured using spectroscopic ellipsometry.

C. FABRICATION OF SHJ SOLAR CELLS

In order to demonstrate a double layered TCO with the IZO + ITO in SHJ solar cells, the optical characteristics of the SHJ solar cells were measured and the weighted reflectance was calculated. Figure 1(a) represents SHJ solar cells with IZO + ITO instead of insulator + ITO. A randomly textured N-type Czochralski Si wafer that had a resistivity of 3.8 Ω-cm was used as a substrate. Intrinsic a-Si:H was deposited prior to the deposition of doped a-Si:H on the front surface and on the back surface. N-type a-Si:H and p-type a-Si:H were deposited on both sides of the solar cells. After that, an ITO of 80 nm was deposited on both sides. The IZO was sputtered on the front side of the SHJ solar cells. The IZO was deposited by RF sputtering from an IZO (99.999 %) in an Ar/O_2 mixture at RT. Based on the simulation result with the IZO/Si wafer, the flow rate of the Ar was maintained to 20 sccm, whereas that of the $O_2$was varied to 1, 4, and 5 sccm because the IZO deposited at these flow rates of the O_2 showed an improvement of J_{SC}.

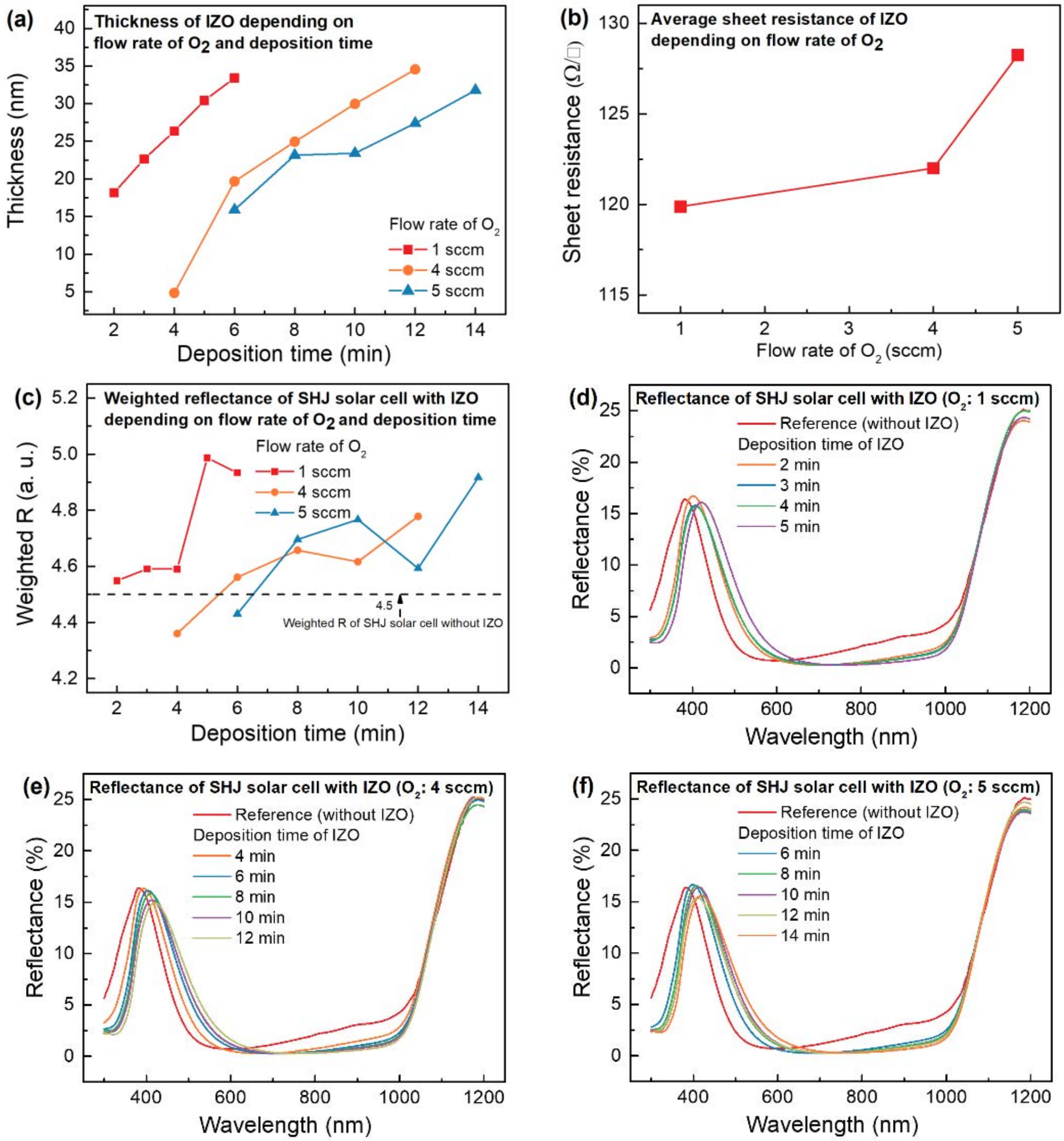

FIGURE 4. (a) Thickness of IZO depending on the flow rate of O_2 and the deposition time. (b) The average sheet resistance of IZO depending on the flow rate of the O_2. (c) Weighted reflectance of the SHJ solar cells with IZO depending on the flow rate of the O_2 and the deposition time. The reflectance of the SHJ solar cells with IZO sputtered at the O_2 flow rate of (d) 1 sccm, (e) 4 sccm, and (f) 5 sccm.

In addition, the deposition time was varied until the thickness of the IZO was below 35 nm. The electrical and deposition rate of the IZO was evaluated depending on the flow rate of O_2 and deposition time. A four-point probe was used to analyze electrical properties, and the thickness of the IZO was measured using spectroscopic ellipsometry. In order to evaluate the feasibility of improving the J_{SC} of SHJ solar cells with IZO + ITO, the reflectance was measured using ultraviolet-visible spectroscopy (UV-VIS). The Rweighted, one of the methods used to examine the J_{SC}, was then first calculated using the optical properties of the SHJ according to the equation $\text{Rweighted} = (\int S\lambda \times R(\lambda) \times \Delta\lambda)/(\int S\lambda \times \Delta\lambda)$.

III. RESULTS AND DISCUSSIONS

We evaluated the thickness and the refractive index (n) of IZO prior to examining the characteristics of the SHJ solar cells with IZO + ITO. Figure 2 shows the thickness and the refractive index of IZO depending on the flow rate of O_2. The trends of the average IZO thickness were decreased and saturated after 4 sccm as the flow rate of the O_2 was increased, as shown in Figure 2(a). The high flow rate of the O_2 was attributed to an increase in the pressure, resulting in a decreased mean free path and energy of sputter particles [19], [20]. In the case of the refractive index, as we induced O_2, the refractive index shifted to a higher value compared to the IZO deposited at

0 sccm. The refractive index of IZO was then shifted toward a negative value by increasing the flow rate of O_2. The shift of the refractive index is caused by the Burstein-Moss effect [14], a phenomenon where the apparent bandgap is higher than the actual bandgap of the semiconductors because the concentration of the electrons exceeds the number of states at the edge of the conduction band. As the concentration of O_2 was increased, the concentration of the free carrier associated with the concentration of O_2 vacancies was decreased, which resulted in a band-edge shift toward a negative value. Due to the decrease of the apparent band gap, the refractive index of IZO might be decreased, which corresponded to the prior literature [14], [21], [22].

In order to examine the feasibility of IZO for solar cells, the photon current densities of Air/ITO/Si and Air/IZO/ITO/Si were evaluated depending on the sputtering condition of IZO, as shown in Figure 3. The reflected photon current (JR), adsorbed photon current in the film (JA), and the adsorbed photon current in the substrate (JG) associated J_{SC} were analyzed, which the incident photon current (JI) was 44 mA/cm^2. The reference structure with Air/ITO/Si was first optimized in order to obtain the highest JG, which resulted in a JG of 40.64 mA/cm^2. Air/IZO/ITO/Si was simulated afterwards, and the optical properties of the IZOs measured using spectroscopic ellipsometry were used. As a result, we observed that the JG of Air/IZO/ITO/Si increased, which is due to a decrease in the JR compared to Air/ITO/Si. We also observed that Air/IZO/ITO/Si with optical properties of IZOs sputtered at the O_2 flow rates of 1, 4, and 5 sccm, which showed a higher JG than the others due to a decrease in JR. The IZOs sputtered at the O_2 flow rates of 1, 4, and 5 sccm showed a higher JA than the IZOs sputtered at the O_2 flow rates of 0, 2, and 3 sccm. The JG of IZOs sputtered at O_2 flow rates of 1, 4, and 5 sccm showed higher rates than the others because the change of the JR is larger than that the change of the JA. Therefore, we showed that IZOs sputtered at the O_2 flow rates of 1, 4, and 5 sccm would show high J_{SC} via OPAL2.

Before evaluating the feasibility of the IZO + ITO for SHJ solar cells, the optical and electrical properties of the IZO sputtered at the O_2 flow rates of 1, 4, and 5 sccm was evaluated depending on the deposition time, as shown in Figure 4(a) and Figure 4(b). Figure 4(a) shows the thickness of the IZO depending on the flow rate of the O_2 and the deposition time. A decrease of the IZO deposition rate was observed by increasing the flow rate of O_2 due to a decrease of the mean free path, which was discussed above. The deposition rates of the IZO at 1, 4, and 5 sccm were 6.1, 3.0, and 2.3 nm/minute. In regard to the sheet resistance of IZO, a noticeable change of the sheet resistance was not observed depending on the thickness, but an increase of the sheet resistance was observed with an increase in the O_2 flow rate. The increase of the sheet resistance by increasing the flow rate of O_2 is commonly shown by the decreasing concentration of O_2 vacancies. The resistivity of the IZO is typically decided by the O_2 vacancies. However, the O_2 flow rate was increased, so the concentration of O_2 vacancies was decreased, which resulted in an increase in resistivity. H. Pan *et al.* also reported that a reduction of the O_2 vacancies caused high resistivity [23].

In order to examine the optical properties of IZO + ITO for SHJ solar cells, the reflectance of SHJ solar cells with IZO + ITO was measured first, as shown in Figure 4(d), Figure 4(e), and Figure 4(f). As a result, the shift of reflectance toward a long wavelength was commonly observed when the thickness of the IZO was increased. In addition, we observed that reflectance on the long wavelength was decreased. These reflectance changes are due to the light that was reflected on the IZO changing the wavelength ranges, which showed destructive and constructive interferences. This mechanism is commonly known as a double-layer anti-reflection coating (DLARC) [11], [24]. In the case of the single-layer anti-reflection coating (SLARC) with ITO, because the total reflection of solar cell was determined by the interference with reflected lights from ITO and Si, in order to obtain a maximum solar light intensity, researchers have been studying minimizing the reflectance at the wavelength near 600 nm by optimizing the thickness and optical characteristics of ITO [25]–[27]. On the other hand, in the case of the DLARC, the total reflection of the solar cell was taken by the interference with reflected lights from IZO, ITO, and Si, resulting in the shift of the reflectance toward a long wavelength. Therefore, even though JR in the range from 400 to 600 nm was increased by increased reflectance in that range, the decrease of JR in the range from 300 to 400 nm and from 600 to 1050 nm was larger, resulting in a lower JR in the case of IZO + ITO.

In order to evaluate the feasibility of IZO + ITO for SHJ solar cells, the solar weighted resistance was calculated as shown in Figure 4(c). The IZO deposited at 4 sccm for 4 minutes and that deposited 5 sccm for 6 minutes both showed lower solar weighted reflectance compared to the SHJ solar cells without IZO. The IZO deposited under conditions showed higher solar weighted reflectance because the reflectance near the wavelength that showed a high intensity of solar light was decreased by over-shifting the reflectance. As a result, we demonstrated that SHJ solar cells with IZO + ITO show less reflectance, which represents that the SHJ solar cells with IZO + ITO improve J_{SC}.

IV. CONCLUSION

This article presents an SHJ solar cell with IZO + ITO that can improve the J_{SC} of an SHJ solar cell. The average thickness and optical properties of IZO, depending on the flow rate of O_2, were evaluated. We observed an increase with the JG using the optical properties of IZO because the IZO was deposited on the ITO via an OPAL2 simulation. In addition, an increase in the sheet resistance of IZO with an increase of the flow rate of O_2 is due to a decrease of O_2. In order to apply IZO on SHJ solar cells, the thickness of IZO was also varied up to 35 nm, and the O_2 flow rates at 1, 4, and 5 sccm were chosen. The shift of reflectance toward a long wavelength manifested as the thickness of IZO was increased. As a result, an SHJ solar cell with an IZO of 4.84 nm deposited with the O_2 flow rate at 4 sccm shows the lowest solar weighted reflectance of 4.36%, which is lower than the SHJ solar cell without IZO. Therefore, we demonstrated that SHJ with IZO/ITO shows a better J_{SC}.

ACKNOWLEDGMENT

(Doowon Lee and Ahreum Lee contributed equally to this work.)

REFERENCES

[1] J. Zhao, A. Wang, and M. A. Green, "24·5% efficiency silicon PERT cells on MCZ substrates and 24·7% efficiency PERL cells on FZ substrates," *Prog. Photovolt., Res. Appl.*, vol. 7, no. 6, pp. 471–474, Nov. 1999.

[2] M. A. Green, "The passivated emitter and rear cell (PERC): From conception to mass production," *Sol. Energy Mater. Sol. Cells*, vol. 143, pp. 190–197, Dec. 2015, doi: 10.1016/j.solmat.2015.06.055.

[3] J. Haschke, O. Dupré, M. Boccard, and C. Ballif, "Silicon heterojunction solar cells: Recent technological development and practical aspects—From lab to industry," *Sol. Energy Mater. Sol. Cells*, vol. 187, pp. 140–153, Dec. 2018, doi: 10.1016/j.solmat.2018.07.018.

[4] S. Y. Herasimenka, W. J. Dauksher, and S. G. Bowden, ">750 mV open circuit voltage measured on 50 μm thick silicon heterojunction solar cell," *Appl. Phys. Lett.*, vol. 103, no. 5, Jul. 2013, Art. no. 053511, doi: 10.1063/1.4817723.

[5] K. Yoshikawa, H. Kawasaki, W. Yoshida, T. Irie, K. Konishi, K. Nakano, T. Uto, D. Adachi, M. Kanematsu, H. Uzu, and K. Yamamoto, "Silicon heterojunction solar cell with interdigitated back contacts for a photoconversion efficiency over 26%," *Nature Energy*, vol. 2, no. 5, p. 17032, May 2017, doi: 10.1038/nenergy.2017.32.

[6] Q. Wang, "Status of crystalline silicon PERC solar cells," in *Proc. NIST/UL Workshop Photovoltaic Mater. Durability*, Gaithersburg, MD, USA, 2019, pp. 12–13.

[7] S. De Wolf and M. Kondo, "Boron-doped a-Si:H/c-Si interface passivation: Degradation mechanism," *Appl. Phys. Lett.*, vol. 91, no. 11, 2007, Art. no. 112109, doi: 10.1063/1.2783972.

[8] Z. C. Holman, A. Descoeudres, L. Barraud, F. Z. Fernandez, J. P. Seif, S. De Wolf, and C. Ballif, "Current losses at the front of silicon heterojunction solar cells," *IEEE J. Photovolt.*, vol. 2, no. 1, pp. 7–15, Jan. 2012, doi: 10.1109/JPHOTOV.2011.2174967.

[9] A. Cruz, F. Ruske, A. Eljarrat, P. P. Michalowski, A. B. Morales-Vilches, S. Neubert, E.-C. Wang, C. T. Koch, B. Szyszka, R. Schlatmann, and B. Stannowski, "Influence of silicon layers on the growth of ITO and AZO in silicon heterojunction solar cells," *IEEE J. Photovolt.*, vol. 10, no. 2, pp. 703–709, Mar. 2020, doi: 10.1109/JPHOTOV.2019.2957665.

[10] A. Cruz, D. Erfurt, P. Wagner, A. B. Morales-Vilches, F. Ruske, R. Schlatmann, and B. Stannowski, "Optoelectrical analysis of TCO+Silicon oxide double layers at the front and rear side of silicon heterojunction solar cells," *Sol. Energy Mater. Sol. Cells*, vol. 236, Mar. 2022, Art. no. 111493, doi: 10.1016/j.solmat.2021.111493.

[11] D. W. Lee, M. F. Bhopal, S. H. Lee, A. R. Lee, H. J. Kim, M. A. Rehman, Y. Seo, K. Lim, W. Shin, and S. H. Lee, "Effect of additional HfO_2 layer deposition on heterojunction c-Si solar cells," *Energy Sci. Eng.*, vol. 6, no. 6, pp. 706–715, Dec. 2018, doi: 10.1002/ese3.245.

[12] A. R. Lee, D. W. Lee, S. H. Lee, M. F. Bhopal, H. J. Kim, K.-J. Lim, W.-S. Shin, S. H. Lee, and J. Kim, "Study of double layer indium tin oxide in silicon hetero-junction solar cells," *J. Nanosci. Nanotechnol.*, vol. 20, no. 1, pp. 161–167, Jan. 2020, doi: 10.1166/jnn.2020.17242.

[13] J. Montero, C. Guillén, and J. Herrero, "AZO/ATO double-layered transparent conducting electrode: A thermal stability study," *Thin Solid Films*, vol. 519, no. 21, pp. 7564–7567, Aug. 2011, doi: 10.1016/j.tsf.2010.12.103.

[14] M. Morales-Masis, S. M. De Nicolas, J. Holovsky, S. De Wolf, and C. Ballif, "Low-temperature high-mobility amorphous IZO for silicon heterojunction solar cells," *IEEE J. Photovolt.*, vol. 5, no. 5, pp. 1340–1347, Sep. 2015, doi: 10.1109/JPHOTOV.2015.2450993.

[15] S. F. Kamino, "Fully textured monolithic perovskite/silicon tandem solar cells with 25.2% power conversion efficiency," *Nature Mater.*, vol. 17, no. 9, pp. 820–826, Sep. 2018, doi: 10.1038/s41563-018-0115-4.

[16] W. Cai, H. Li, and Z. Zang, "One-volt, solution-processed InZnO thin-film transistors," *IEEE Electron Device Lett.*, vol. 42, no. 4, pp. 525–528, Apr. 2021, doi: 10.1109/LED.2021.3062422.

[17] W. Cai, H. Li, M. Li, and Z. Zang, "Performance enhancement of solution-processed InZnO thin-film transistors by al doping and surface passivation," *J. Semicond.*, vol. 43, no. 3, Mar. 2022, Art. no. 034102, doi: 10.1088/1674-4926/43/3/034102.

[18] W. Cai, Z. Zang, and L. Ding, "Self-assembled monolayers enhance the performance of oxide thin-film transistors," *J. Semicond.*, vol. 42, no. 3, Mar. 2021, Art. no. 030203, doi: 10.1088/1674-4926/42/3/030203.

[19] V. Assuncao, E. Fortunato, A. Marques, H. Aguas, I. Ferreira, M. E. V. Costa, and R. J. T. Martins, "Influence of the deposition pressure on the properties of transparent and conductive ZnO: Ga thin-film produced by RF sputtering at room temperature," *Thin Solid Films*, vol. 427, nos. 1–2, pp. 401–405, 2003, doi: 10.1016/S0040-6090(02)01184-7.

[20] M. Al-Mansoori, S. Al-Shaibani, A. Al-Jaeedi, J. Lee, D. Choi, and F. S. Hasoon, "Effects of gas flow rate on the structure and elemental composition of tin oxide thin films deposited by RF sputtering," *AIP Adv.*, vol. 7, no. 12, Dec. 2017, Art. no. 125105, doi: 10.1063/1.5001883.

[21] T. Moss, "The interpretation of the properties of indium antimonide," *Proc. Phys. Soc. Sect. B*, vol. 67, no. 10, p. 775, 1954, doi: 10.1088/0370-1301/67/10/306.

[22] E. Burstein, "Anomalous optical absorption limit in InSb," *Phys. Rev. Lett.*, vol. 93, p. 632, Feb. 1954, doi: 10.1103/PhysRev.93.632.

[23] H.-C. Pan, M.-H. Shiao, C.-Y. Su, and C.-N. Hsiao, "Influence of sputtering parameter on the optical and electrical properties of zinc-doped indium oxide thin films," *J. Vac. Sci. Technol. A, Vac., Surf., Films*, vol. 23, no. 4, pp. 1187–1191, Jul. 2005, doi: 10.1116/1.1924473.

[24] J. Zhao, A. Wang, P. Altermatt, and M. A. Green, "Twenty-four percent efficient silicon solar cells with double layer antireflection coatings and reduced resistance loss," *Appl. Phys. Lett.*, vol. 66, no. 26, pp. 3636–3638, Jun. 1995.

[25] D. Bouhafs, A. Moussi, A. Chikouche, and J. M. Ruiz, "Design and simulation of antireflection coating systems for optoelectronic devices: Application to silicon solar cells," *Sol. Energy Mater. Sol. Cells*, vol. 52, nos. 1–2, pp. 79–93, 1998, doi: 10.1016/S0927-0248(97)00273-0.

DOOWON LEE received the Ph.D. degree in electrical engineering from Sejong University, Seoul, South Korea, in 2020. He is currently a Postdoctoral Researcher of electrical engineering with Sejong University. His current research interest includes electrical/optical semiconductor devices.

AHREUM LEE received the B.S. and M.S. degrees in electrical engineering from Sejong University, Republic of Korea, in 2018 and 2020, respectively. Her current research interest includes electrical/optical semiconductor devices.

HEE-DONG KIM received the B.S., M.S., and Ph.D. degrees in electrical engineering from Korea University, Republic of Korea, in 2007, 2009, and 2014, respectively. From 2014 to 2015, he was a Postdoctoral Fellow with the Department of Technology, Leibniz-Institut für Innovative Mikroelektronik (IHP), Germany. He is currently an Associate Professor with the Department of Electrical Engineering, Sejong University, Republic of Korea. His current research interests include electrical/optical semiconductor devices and nonvolatile memory devices.